

Article

Valorization of Hazardous Organic Solid Wastes towards Fuels and Chemicals via Fast (Catalytic) Pyrolysis

Kyriazis C. Rekos ^{1,2}, Ioannis D. Charisteidis ¹, Evangelos Tzamos ³, Georgios Palantzas ⁴,
Anastasios I. Zouboulis ¹ and Konstantinos S. Triantafyllidis ^{1,2,*}

- ¹ Department of Chemistry, Aristotle University of Thessaloniki, 54124 Thessaloniki, Greece; rkyriazi@chem.auth.gr (K.C.R.); icharisteidis@gmail.com (I.D.C.); zoubouli@chem.auth.gr (A.I.Z.)
² Center for Interdisciplinary Research and Innovation (CIRI-AUTH), Aristotle University of Thessaloniki, 57001 Thessaloniki, Greece
³ R & D Department, North Aegean Slops S.A., 26 Oktovriou Str. 42, 54627 Thessaloniki, Greece; tzamos@chem.auth.gr
⁴ Department of Civil Engineering, Faculty of Engineering, Aristotle University of Thessaloniki, 54124 Thessaloniki, Greece; palantzas@civil.auth.gr
* Correspondence: ktrianta@chem.auth.gr

Abstract: The management of municipal and industrial organic solid wastes has become one of the most critical environmental problems in modern societies. Nowadays, commonly used management techniques are incineration, composting, and landfilling, with the former one being the most common for hazardous organic wastes. An alternative eco-friendly method that offers a sustainable and economically viable solution for hazardous wastes management is fast pyrolysis, being one of the most important thermochemical processes in the petrochemical and biomass valorization industry. The objective of this work was to study the application of fast pyrolysis for the valorization of three types of wastes, i.e., petroleum-based sludges and sediments, residual paints left on used/scrap metal packaging, and creosote-treated wood waste, towards high-added-value fuels, chemicals, and (bio)char. Fast pyrolysis experiments were performed on a lab-scale fixed-bed reactor for the determination of product yields, i.e., pyrolysis (bio)oil, gases, and solids (char). In addition, the composition of (bio)oil was also determined by Py/GC-MS tests. The thermal pyrolysis oil from the petroleum sludge was only 15.8 wt.% due to the remarkably high content of ash (74 wt.%) of this type of waste, in contrast to the treated wood and the residual paints (also containing 30 wt.% inorganics), which provided 46.9 wt.% and 35 wt.% pyrolysis oil, respectively. The gaseous products ranged from ~7.9 wt.% (sludge) to 14.7 (wood) and 19.2 wt.% (paints), while the respective solids (ash, char, reaction coke) values were 75.1, 35, and 36.9 wt.%. The thermal (non-catalytic) pyrolysis of residual paint contained relatively high concentrations of short acrylic aliphatic ester (i.e., n-butyl methacrylate), being valuable monomers in the polymer industry. The use of an acidic zeolitic catalyst (ZSM-5) for the in situ upgrading of the pyrolysis vapors induced changes on the product yields (decreased oil due to cracking reactions and increased gases and char/coke), but mostly on the pyrolysis oil composition. The main effect of the ZSM-5 zeolite catalyst was that, for all three organic wastes, the catalytic pyrolysis oils were enriched in the value-added mono-aromatics (BTX), especially in the case of the treated wood waste and residual paints. The non-condensable gases were mostly consisting of CO, CO₂, and different amounts of C₁–C₄ hydrocarbons, depending on initial feed and use or not of the catalyst that increased the production of ethylene and propylene.

Keywords: solid organic waste valorization; residual paints; creosote-treated wood; petroleum sludge; pyrolysis; catalytic fast pyrolysis; bio-oil; monomers; BTX aromatics; char

1. Introduction

The management of municipal and industrial organic solid wastes has become one of the most crucial environmental problems in modern societies. According to the European



Citation: Rekos, K.C.; Charisteidis, I.D.; Tzamos, E.; Palantzas, G.; Zouboulis, A.I.; Triantafyllidis, K.S. Valorization of Hazardous Organic Solid Wastes towards Fuels and Chemicals via Fast (Catalytic) Pyrolysis. *Sustain. Chem.* **2022**, *3*, 91–111. <https://doi.org/10.3390/suschem3010007>

Academic Editor: Michael T. Timko

Received: 20 January 2022

Accepted: 24 February 2022

Published: 25 February 2022

Publisher's Note: MDPI stays neutral with regard to jurisdictional claims in published maps and institutional affiliations.



Copyright: © 2022 by the authors. Licensee MDPI, Basel, Switzerland. This article is an open access article distributed under the terms and conditions of the Creative Commons Attribution (CC BY) license (<https://creativecommons.org/licenses/by/4.0/>).

Commission Directive 2008/98/EC, it is mentioned that “the following waste hierarchy shall apply as a priority order in waste prevention and management legislation and policy: prevention; preparing for reuse; recycling; other recovery, e.g., energy recovery; and finally, disposal”. Thus, when the re-use of waste materials is not possible, the recycling of organic wastes via conversion to their primary building blocks or derivative high-value-added chemicals and fuels should be applied [1]. Still, when the recovery of chemicals is not efficient enough, the waste to energy path is applied via combustion/incineration or gasification and subsequently via steam production or steam/electricity co-generation for improving energy recovery [2,3]. However, there is very little knowledge concerning hazardous organic waste management, and the method of incineration towards energy production has already been in dispute [4]. Over the last few years, Greece, in accordance with EU regulations, put forward the “National Waste Management Plan (ESDA)” in 2015 and later, in 2016, the “National Hazardous Waste Management Plan (ESDEA)”, which were formulated by the Ministry of Environment and Energy with the aim to set out the strategy, objectives, and actions for waste management at the national level.

To this end, pyrolysis, being one of the most important thermochemical processes in the petrochemical industry, may offer a solution to the sustainable management of hazardous organic solid wastes [5]. More specifically, fast pyrolysis of organic feedstocks/wastes, such as biomass wastes, leads to enhanced production of liquid product (pyrolysis oil), which can reach up to 70–80 wt.%, along with the co-produced char and gases (mainly CO, CO₂, and methane). The pyrolysis oil can serve as a pool of various value-added chemicals (e.g., phenolics) or can be upgraded downstream via hydrotreatment processes towards drop-in hydrocarbon biofuels or bio-crude to be co-processed with petroleum fractions in conventional refineries [6–9].

In fast pyrolysis, the solid feed is heated to relatively moderate/high temperatures (400–700 °C) with high heating/cooling rates under inert atmosphere in the absence of oxygen, aimed at the increased production of pyrolysis oil, which, in the case of lignocellulosic biomass (wood or agricultural waste), is rich in phenolics, containing also acetic acid, ketones, aldehydes, ethers, esters, furans, aliphatics, and aromatics (up to ca. 75 wt.% based on initial feed). Non-condensable gases are also produced (10–20 wt.%; CH₄, CO₂, CO) as well as char (10–25 wt.%) [10–15]. The wood-derived pyrolysis oil (bio-oil) can be upgraded in situ by catalytic fast pyrolysis (CFP). In CFP, the initially formed thermal pyrolysis vapors undergo deoxygenation reactions thus producing a less oxygenated bio-oil [16–21]. Acidic zeolites are usually applied, with ZSM-5 zeolite being the most representative, which induce cracking, de-alkoxylation, (de)alkylation, aromatization, condensation, and oligomerization reactions of the intermediate pyrolysis vapors, leading to the production of a highly aromatic bio-oil, comprising of mono-aromatic hydrocarbons (BTX) and naphthalenes [10,11,22,23]. The reaction mechanisms and the effect of ZSM-5 and other zeolites' characteristics on bio-oil upgrading and production of aromatics in catalytic fast pyrolysis of lignocellulosic biomass have been extensively studied in the past [24–31].

Petroleum-containing sludges are usually recovered at high quantities at refineries, liquid fuel tanks, ship bunkers, and sewage treatment plants. Recent literature suggests management techniques such as incineration, photo-catalysis, bio-degradation, and pyrolysis [32,33]. However, due to their very inconsistent composition (poly-aromatic hydrocarbons, heavy metals, inorganic salts, and humidity) the most commonly applied management technique is incineration [34]. Still, there are some very serious disadvantages when employing this method, such as the high humidity of the sludge (water removal of the sludge prior to incineration is required, but is very costly) [35], the hazardous toxic gases formed during incineration [36], and the high ash and metal residue volumes formed, which need further management [32]. On the other hand, Liu et al. studied the pyrolysis of these sludges at 325–450 °C, on a fluid bed reactor [37,38] and suggested that it is possible to recover almost ~80% of the total carbon of the initial feed as useful pyrolytic products. The pyrolytic oil recovered, which represents up to ~30–50% of the total products, consists of poly-aromatic compounds and diesel-type hydrocarbons, which can be separated with

distillation and used as chemicals or fuels [39]. The non-condensable gaseous products recovered were mainly consisting of CO and CO₂ και light hydrocarbons and represented up to ~10–20% of the total products. The produced char (solid products) made up to ~30–50% of the total products and had a high surface area, which consequently can be used to absorb the metals of the initial feed [40,41].

The recycling of scrap metal wastes can be quite profitable, especially in the most industrially advanced economies [42]. However, in the case of scrap metal coated with paint residues, in order to remove the paint residues and recover the metal, the most commonly known technique is incineration (co-producing energy), which, however, leads to the production of toxic gas emissions that require further management costs, making the process financially unsustainable. Thus, in most cases these wastes are deposited in high quantities on landfills [43], which is considered very toxic towards the environment and human health because the paint residues contain high amounts of aromatic hydrocarbons, such as benzene, toluene, xylene, etc., which are widely considered to be carcinogens when inhaled [44]. Yet there is still very little literature concerning this type of waste material. To this end, David et al. studied the metal recovery of paint containing aluminum canisters through slow pyrolysis at 580 °C [45]. The suggested process took place in two steps. First, the feed was slowly pyrolyzed towards char and light gases, and then the char-containing metal was incinerated with air to produce energy and recover the “paint free” scrap metal. It was, however, concluded that tuning of the pyrolysis conditions is necessary to maximize the metal recovery efficiency.

Creosote-containing wood waste is usually accumulated from previously used railway tiles or utility pillars [46]. Creosote is a tar-based mixture of substances that is impregnated to the wood as a preservative and is very resistant to insects, birds, and aging [47]. However, after several years of usage the creosote-containing wood materials are replaced with new ones, leading to excessive amounts of hazardous wood wastes. This type of waste material is considered hazardous because it contains high concentrations of phenolic and poly-aromatic compounds (such as naphthalenes and anthracenes), which are considered highly carcinogenic [46]. As a matter of fact, simple deposition of these wastes to landfills is nowadays under dispute. In order to provide more insight on the sustainable management of this type of wastes, Kim et al. studied the thermal, fluid bed pyrolysis of creosote-impregnated wood wastes that were previously used as railway wood tiles [48]. It was found that the pyrolytic oil yield was maximized at the reaction temperature of ~450 °C and was ~69 wt.% of the initial feed. Meanwhile, at the same temperature, the gas yield was found to be ~10 wt.%, and the char yield was ~21 wt.%. The pyrolytic oil was easily separated to two phases, which represented the wood-based (bio)oil and the creosote-based pyrolytic oil. Water analysis of these phases pointed out that while wood-based (bio)oil was consisting of ~65% aquatic phase (the rest ~35% being organic), the creosote-based pyrolytic oil was totally organic based. As a matter of fact, the higher heating value (HHV) of the wood-based (bio)oil was found to be ~11 MJ/kg, while the HHV of the creosote-based pyrolytic oil was ~39 MJ/kg. Further analysis with GC-MS pointed out that wood-based (bio)oil was mostly consisting of phenols and oxy-phenols, while the creosote-based pyrolytic oil was mainly consisting of poly-aromatic compounds. The main gas products were CO and CO₂, as well as small amounts of CH₄ and H₂, while their high heating value was ~8 MJ/kg. The HHV of char was found to be ~36 MJ/kg, which is considered to be a good value for solid fuels [48,49].

The main objective of this work is to study the application of fast pyrolysis in the conversion of hazardous organic wastes towards high-value-added chemicals. The type of wastes under investigation comprised of petroleum-based sludges, residual paints left on used/scrap metal packaging, and treated wood waste that has been impregnated with hazardous substances, i.e., creosote, for conservation purposes. The amounts of these wastes in Greece are estimated to be approximately 1000 tons per year for petroleum sludges, 800 tons per year for residual paint metal containers, and 10 tons per year for impregnated timber, originating from wooden poles of the electricity distribution networks,

the above-ground telecommunication network, but also from the sleepers of the railway network. Emphasis is placed on the in situ upgrading of the pyrolysis oils with the use of an acidic zeolite catalyst (ZSM-5). Such types of wastes, especially the two latter ones, have not been previously systematically investigated as potential feedstocks in fast (catalytic) pyrolysis. More specifically, it is shown that methacrylates and oxy/alkyl-phenols can be recovered by the fast pyrolysis of paints and treated wood, respectively, while xylene and other BTX mono-aromatics and naphthalenes can be obtained from the catalytic pyrolysis (in situ bio-oil upgrading) of treated wood and paints. Additionally, the non-condensable gases may be used as direct “fuels” or sources of ethylene/propylene (in the case of catalytic fast pyrolysis), and the char produced can be used as soil remediation agent or as the basis of porous activated carbons.

2. Materials and Methods

2.1. Raw Materials—Feeds

The solid waste materials that were tested are shown in Figure 1. These are: (a) petroleum-containing sludges and sediments that were collected from the bottom of ship bunkers (NAS-1), (b) scrap metal paint residues that were collected as leftovers from marine paint-containing canisters (NAS-2) (the residual paint was removed (scratched) from the metal surface and was further used for characterization and pyrolysis tests), and (c) utility wood waste that were impregnated with creosote for conservation purposes (NAS-3). These three wastes were kindly provided by North Aegean Slops S.A., Thessaloniki, Greece.



Figure 1. Waste materials, (a): Petroleum containing sludge (NAS-1), (b): Scrap metal paint residue (NAS-2), and (c): Creosote-treated wood (NAS-3).

For the catalytic pyrolysis tests, a commercial ZSM-5 zeolite (Zeolyst, CBV 8014) with a Si/Al ratio equal to 40 was used. As the zeolite was received in its ammonium form, it was converted to the proton form, H-ZSM-5, via calcination in air, for 3 h at 500 °C. Detailed characterization results of this catalytic material have already been reported by Lazaridis et al. [11].

2.2. Raw Materials Physicochemical Properties

The water content of the waste materials was measured with the ASTM D 3173—03 method. In brief, the weight loss upon heating the materials (equilibrated at room conditions for 2 weeks) at 105 °C, for 24 h, represented the humidity content. Similarly, the ash content was determined with the ASTM E-1755-01 method, as the solid residue of the dried (at 105 °C, 24 h) waste materials that were heated in air at 575 °C for 3 h.

The elemental CHNS analysis of the solid wastes was determined on a EuroEA 3000 elemental analyzer (EuroVector SpA, Pavia, Italy). The oxygen content was calculated by difference: %O = 100 – %ash – %C – %H – %N – %S (corresponding to the organic O content). The higher heating value (HHV) of the samples was determined by measuring

the gross heat of combustion energy, using a Parr 1261 bomb calorimeter (Parr Instrument Co., Moline, IL, USA), based on the ASTM D 4809 method. Additionally, a theoretical calculation of HHV was performed from the elemental analysis results, using the following equation (Equation (1)) [50,51]:

$$\text{HHV} = 0.35160 \text{ C} + 1.16225 \text{ H} - 0.11090 \text{ O} + 0.06280 \text{ N} + 0.10465 \text{ S} \quad (1)$$

The waste materials were also characterized by Fourier-transform infrared spectroscopy on an FTIR spectrometer (model FTIR-2000, Perkin Elmer, Waltham, MA, USA) using the KBr dilution method. All spectra were collected from 450 to 4000 cm^{-1} with 4 cm^{-1} resolution (10 co-added scans) and were baseline corrected and converted into transmittance mode. Scanning electron microscopy–energy dispersive spectroscopy (SEM–EDS) analysis of the solid wastes was performed on a JEOL 6300 equipped with X-ray microanalysis (OXFORD ISIS 2000).

The thermal stability and decomposition profile of the waste materials was determined by thermogravimetric analysis (TGA) experiments, using a STA 449 F5 Jupiter instrument (Netzsch, Germany). The samples were heated under N_2 flow (100 cc/min), in the temperature range of 25 to 900 $^\circ\text{C}$ and at a heating rate of 10 $^\circ\text{C}/\text{min}$.

2.3. Fast Pyrolysis Experiments on the Py/GC-MS System

The thermal and the catalytic fast pyrolysis experiments of the three NAS dried solid wastes were performed on a Multi-Shot Micro-Pyrolyzer (EGA/PY-3030D, Frontier Laboratories, Fukushima, Japan) connected to a gas chromatograph-mass spectrometer system (GCMSQP2010, Shimadzu), which is shown in Supplementary Material, Figure S1 and in more detail in our previous works [11]. In a typical thermal (non-catalytic) run, a dried (105 $^\circ\text{C}$ for 24 h) mixture of 1 mg NAS waste and 3 mg silica sand (as inert heat carrier material) were loaded into a stainless-steel cup, which was instantaneously dropped in the hot reactor/furnace, and pyrolysis was conducted at the preset temperatures of 600 $^\circ\text{C}$ for 12 s. In the catalytic fast pyrolysis experiments, 1 mg of dried NAS waste was mixed with 3 mg of the dried H-ZSM-5 (catalyst to feed ratio 3:1). Helium (99.999%) was employed as the carrier gas at a flow rate of 100 mL min^{-1} in a micropyrolyzer, with an injector split ratio of 1:150 and 1 mL min^{-1} in the GC column. A capillary column was used (MEGA-5 HT) with the stationary phase consisting of 5% diphenyl and 95% dimethylpolysiloxane (30 $\text{m} \times 0.25 \text{ mm}$ and 0.25 μm film thickness). The GC oven was programmed at a 4 min hold at 40 $^\circ\text{C}$ followed by heating (5 $^\circ\text{C min}^{-1}$) up to 300 $^\circ\text{C}$, where it was held constant for 7 min. The injector and detector temperature were kept at 300 $^\circ\text{C}$. The mass spectra were recorded in the range of m/z 45 to 500, with a scan speed of 5000 amu/s . Identification of mass spectra peaks was achieved using the scientific library NIST11s. The derived compounds were classified in the following 16 groups: monoaromatics (AR), aliphatics (ALI), phenols (PH), acids (AC), esters (EST), alcohols (AL), ethers (ETH), aldehydes (ALD), ketones (KET), polycyclic aromatic hydrocarbons (PAH's), sugars (SUG), nitrogen compounds (NIT), sulfur compounds (SUL), oxygenated aromatics (OxyAR), oxygenated phenols (OxyPH), and unidentified compounds (UN). At least three experiments were performed for each solid waste sample, and the reported data of the relative abundance of each compound is the mean value with a standard deviation being below 10% in all cases.

2.4. Fast Pyrolysis Experiments on Bench-Scale Fixed-Bed Reactor

The thermal and catalytic fast pyrolysis experiments of dried solid wastes were also performed on a bench-scale fixed-bed tubular reactor (Supplementary Material, Figure S2). The experimental procedure is described in detail in our previous work [11]. In brief, the solid waste samples were inserted from the top of the reactor instantaneously, with the aid of a specially designed piston, to the preheated reactor zone and were pyrolyzed at 600 $^\circ\text{C}$ on a hot quartz-wool layer placed on top of the silica sand (non-catalytic experiments) or the catalyst bed. The produced pyrolysis vapors were driven downwards through the sand

or catalyst bed with the aid of a constant N₂ flow (100 cm³/min) for 20 min. The pyrolysis vapors exiting the reactor were condensed in pre-weighted spiral glass receivers that were placed in a cooling bath at −15 °C. The pyrolysis oil was collected with methanol and was analyzed by GC-MS (GCMS-QP2010, Shimadzu) with analysis parameters described above for the Py/GC-MS system. The NIST11s mass spectral library was used for the identification of the compounds in the pyrolysis oil, which were categorized in 16 groups as for the Py/GC-MS experiments. The water content of the pyrolysis oils was determined by Karl–Fischer titration (ASTM E203-08), while the elemental analysis (C/H/N/S) was determined by LECO 628 and LECO 932 analyzers (St. Joseph, MI, USA); O was determined by difference.

The non-condensable gases were collected and analyzed in a HP 5890 series II, equipped with four columns, i.e., OV101 2ft 1/8' SS, Porapak N 6ft 1/8' SS, Molecular Sieve 5A 6ft 1/8' SS, Poraplot Al₂O₃/KCl 50 m 0.32 mm ID 5 μm, and two detectors (TCD and FID). The carrier gas was He, with a flow rate of 25 mL/min for the TCD and 3 mL/min for the FID. The oven parameters were 40 °C initial temperature for 1 min, to 110 °C (isothermal for 5 min) with a heating rate of 10 °C/min, and then to 190 °C (isothermal for 5 min) with a heating rate of 15 °C/min. The following gases were quantitatively determined using external standard gas mixtures: H₂, O₂, N₂, CO₂, CO, and light hydrocarbons from CH₄ to C₆. The amount of solids, which consisted of char in the non-catalytic pyrolysis experiments, or char plus coke-on-catalyst in the catalytic pyrolysis experiments, was determined by direct weighing. An indirect estimation of the coke formed on the catalyst, as wt.% on initial feed, was performed by subtracting the measured char content of the non-catalytic experiment from the char + coke content of the catalytic experiments (char formation is not affected by the presence of the catalysts, as feed and catalysts do not come in direct contact). The standard deviation of the product yield values was less than 5%.

3. Results & Discussion

3.1. Waste Materials Physicochemical Properties

The water content and ash content of the three organic solid wastes are presented in Table S1. As previously mentioned in the literature, the most crucial issues towards the sustainable management of petroleum-containing sludges are the high water content [52] and the high ash amount [32], which is in agreement with the results of the present study. More specifically, it is found that the water content of the initial petroleum sludge waste (NAS-1) is ~44.5 wt.%, with the ash content being ~73.6 wt.% (on dry basis). The water has been accumulated in the sludge over time from the water impurities in the fuels stored in the tank or from the water used to clean the tank and collect the sludge. The very high ash content of this waste is probably due to the dust or soil sediments at the bottom of the tank. The composition of the ash is discussed in more detail below. Residual paint on scrap metal (NAS-2) contains a very low amount of water, up to ~3.6 wt.%. The ash content of this waste materials was found to be up to ~30.4 wt.%. This high ash content is maybe due to the additives that are being used at the synthesis of these paints. Creosote-containing wood (NAS-3) contained up to ~9 wt.% of water and its ash content was very low, i.e., ~1.5 wt.%, both of which attributed to the woody nature of the waste.

The semi-quantitative composition of the ash the three waste materials was determined via SEM–EDS. Representative SEM images and EDS spectra are presented in Figure 2, and the EDS results are given in Supplementary Material, Table S2. The data in Table S2 show that the ash of NAS-1 contains a high percentage of Ca and Si, which in combination with the relatively high Al content, probably comes from dust/soil (clays) deposited in the bottom of the petroleum tanks. Additionally, the high Fe content may be due to tank corrosion. The ash of NAS-2 waste contains a very high percentage of Ca, followed by Si, which are attributed to inorganic additives that are used for the synthesis of the paints and pigments to improve their application characteristics and properties (such as CaCO₃, which is used as an additive to improve the shine/glow of the paints) [53]. The ash of NAS-3

waste contains typical elements of wood (lignocellulosic biomass), such as Na, Mg, Si, K, etc., with a high concentration of Ca. The remarkable high content of S probably originates from the creosote preservative [54].

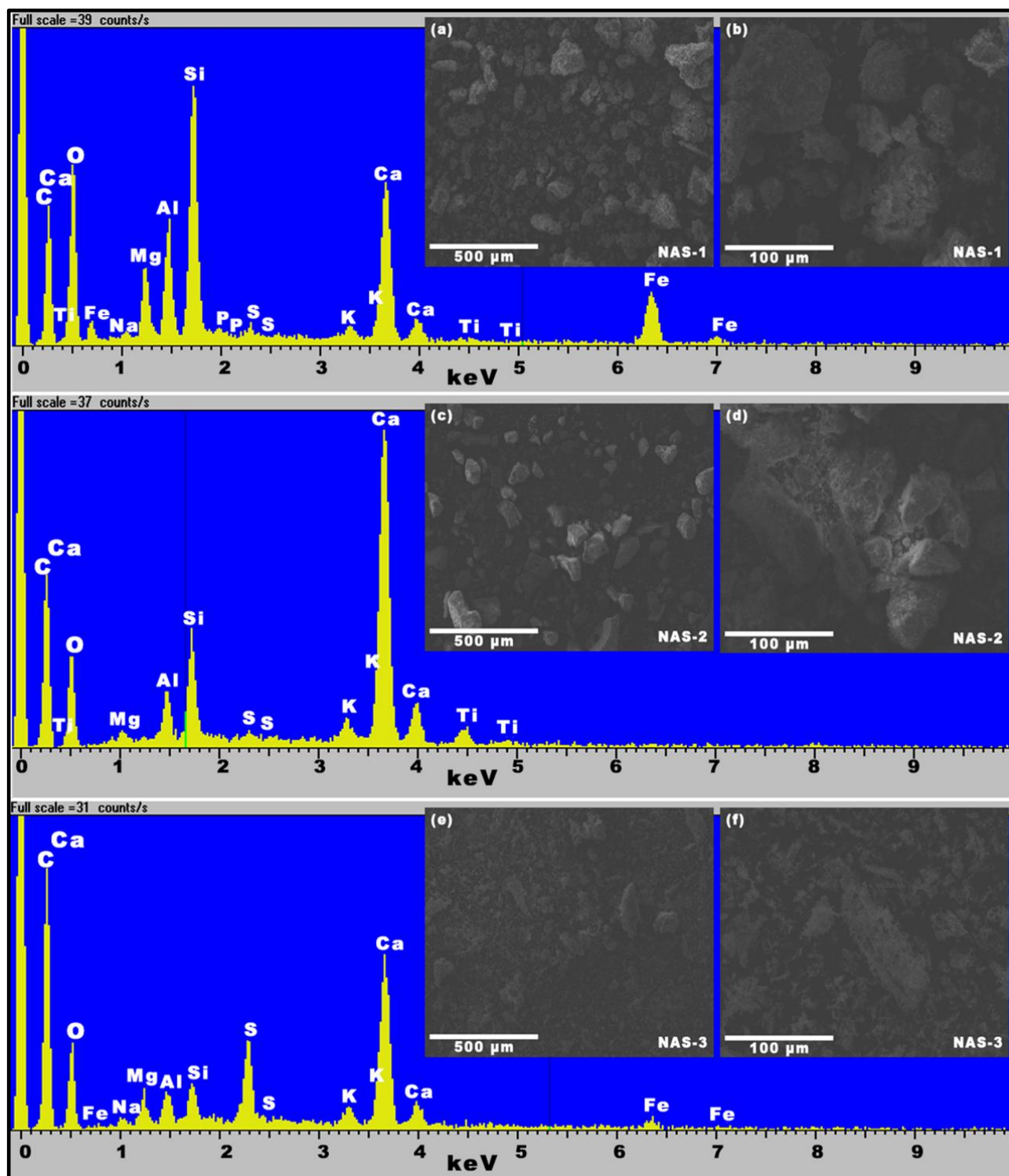


Figure 2. Representative ash EDS spectra of NAS-1, NAS-2, and NAS-3. Insets: SEM images of the ash of NAS-1 (a,b), NAS-2 (c,d), and NAS-3 (e,f).

The results of the elemental C/H/N/S analysis are presented in Table 1, and the normalized values considering the ash content of the solid wastes are presented in

Supplementary Material, Table S3. The NAS-1 waste contains only 15 wt.% C and 1.3 wt.% H due to the high amount of inorganics based on ash determination (~74 wt.%) discussed above. The C/H ratio is ~11.5, which is representative for hydrocarbon mixtures consisting mainly of aromatic hydrocarbons, e.g., the C/H weight ratio for benzene is equal to 12, and for hexadecane it is equal to 5.6. It also contains small amounts of N and S (0.35 and 1.10 wt.%, respectively). When the content of C/H/N/S is normalized on the weight of the organic fraction of NAS-1, then these values increase to 57.8, 5.1, 1.3, and 4.2 wt.% (Supplementary Material, Table S3), being representative of heavy petroleum fractions. The C and H contents of NAS-2 are 48.6 wt.% and 6.2 wt.%, respectively (69.8 and 8.9 wt.% based on organic matter after normalization with the high ash content of ~30 wt.%) and the C/H weight ratio is 7.8. The C and H contents of NAS-3 (50.4 and 5.6 wt.%, respectively) and the corresponding C/H ratio of 9 are close to those of woody lignocellulosic biomass, e.g., for beech wood the corresponding values are 49.4 wt.%, 7.1 wt.%, and 6.9 wt.%, respectively [55]. The slightly higher C/H weight ratio (lower H content) of NAS-3 is due to the presence of creosote, which consists of (poly)phenolic/aromatic compounds [56–58]. In the case of NAS-3, the ash content is low (<1.5 wt.%), so the measured C/H/N/S data represent the elemental analysis of the whole organic solid waste.

Table 1. Elemental analysis of waste materials and theoretical HHV values (relative standard deviation 5%).

Waste	C (% w.t.)	H (% w.t.)	N (% w.t.)	S (% w.t.)	O (% w.t.)	HHV (MJ/kg)	
						Theoretical	Experimental
NAS-1	15.04	1.32	0.35	1.10	8.19 ^(a)	6.05	5.90
NAS-2	48.58	6.17	0.10	0.45	14.70 ^(b)	22.67	21.97
NAS-3	50.37	5.64	0.95	5.60	35.94 ^(c)	20.92	20.95

^(a) The data shows the elemental C/H/N/S analysis results of NAS-1 waste material, which contains very high amounts of inorganics/ash (~74 wt.%). The O was estimated by difference ((100–74)—C/H/N/S); this value maybe overestimated due to the presence of minerals or metal (hydro)oxides in the ash. ^(b) The data shows the elemental C/H/N/S analysis results of NAS-2 waste material, which contains high amounts of inorganics/ash (~30 wt.%). The O was estimated by difference ((100–30)—C/H/N/S); this value maybe overestimated due to the presence of metal oxides in the ash. ^(c) The ash content of NAS-3 is low (<1.5%); thus, the C/H/N/S data represent the actual elemental composition of the organic waste material. The O was estimated by difference ((100–1.5)—C/H/N/S).

The theoretical HHV values, calculated from the elemental analysis data using Equation (1), as well as experimental HHV values, are presented in Table 1. It is noteworthy that the theoretical calculation of HHV of all three wastes, based on elemental analysis, gives values similar to those measured by the calorimeter. It is observed that the HHV of the petroleum sludge (NAS-1) is very low, despite the petroleum oil nature of this organic waste, due to the high content of ash (74 wt.%). If the HHV value is normalized based on the organic matter content of the residue, then it is increased to 25 MJ/kg, which is still less than the typical HHV values of petroleum fuels, e.g., diesel, gasoline, gas-oil (40–45 MJ/kg) [59]. This may be attributed to the large amounts of inorganics that can act as combustion retardants. The hydrocarbon nature of the paints (NAS-2), which contains both aromatic and linear hydrocarbons, e.g., esters, included a moderate HHV value of ~22 kJ/kg (~32 MJ/kg when normalized based on organic matter considering the 30 wt.% ash of this residue). The HHV of NAS-3 (with very low ash content) is ~21 MJ/Kg and is similar to that of pure beech wood (~19 MJ/kg) [60] or olive husk (~21.6 MJ/Kg) [61]. Additionally, the presence of creosote (HHV ~35 MJ/kg [16]) contributes to the HHV of NAS-3.

The FT-IR spectra of the three wastes are presented in Figure 3. Additionally, the assignment of the identified bands is presented in Supplementary Material, Table S4.

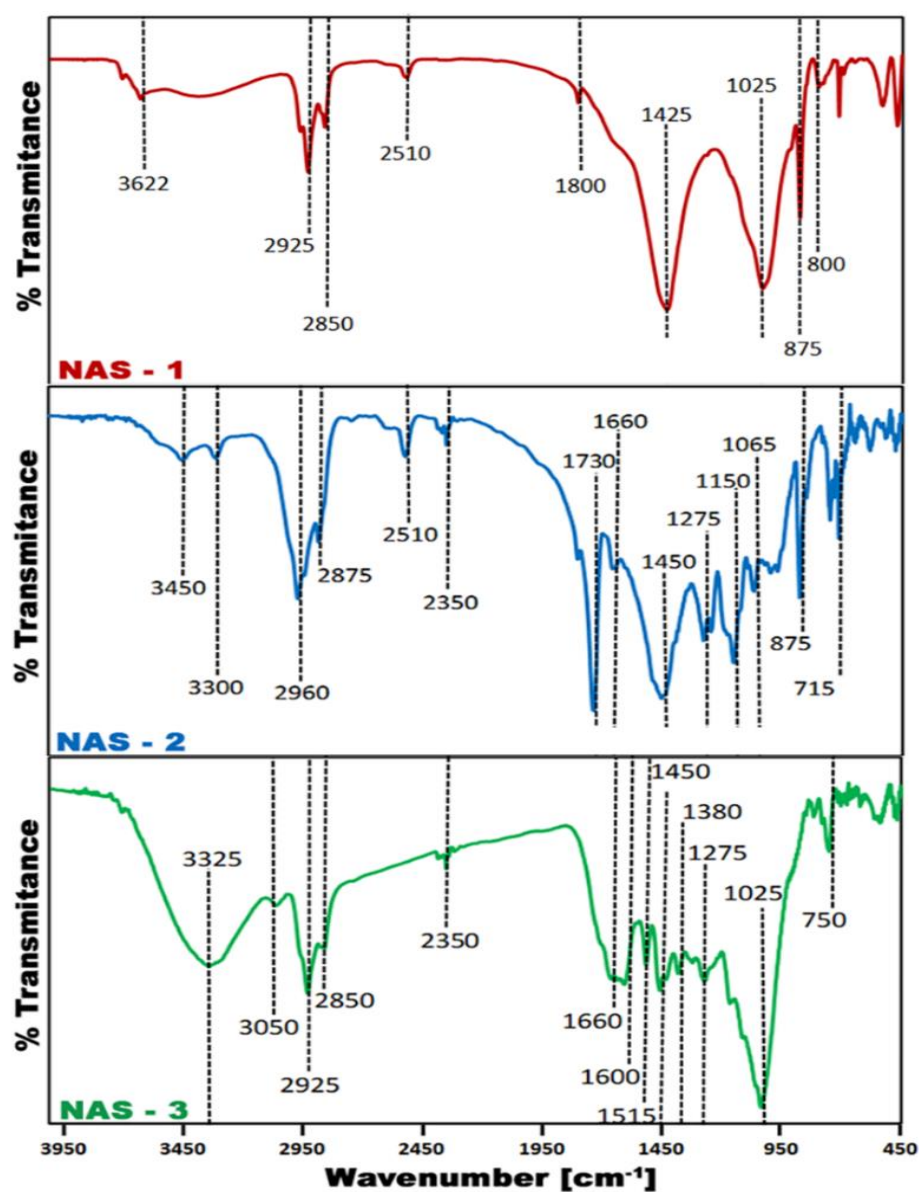


Figure 3. FT-IR spectra of the three waste materials.

The spectra of NAS-1 exhibit bands owing to hydrocarbons of heavy petroleum fractions as well as to the inorganics (clays) contained in this sample. The bands at 2925 cm^{-1} and 2850 cm^{-1} correspond to the C-H asymmetric and symmetric stretching vibrations of the CH_2 groups, respectively, of alkane chains. The band at 2510 cm^{-1} is related to the sulfur content of the sludge (S-H stretching of thiol groups). The strong band at 1425 cm^{-1} is attributed to bending vibrations of the CH_2 and CH_3 groups, and the band at 1025 cm^{-1} is attributed to the Si-O-Si stretching vibrations, which is characteristic for the clay and related (alumino)silicate structures. The bands at 875 and 800 cm^{-1} are related to C-H bending in tri/tetrasubstituted aromatic compounds [62]. The residual paints of NAS-2 are of acrylic type, according to the producer MSDS and technical data sheet [63,64]. The bands at $\sim 3450\text{ cm}^{-1}$ are due to the stretching vibrations of the hydroxyl groups (O-H) of alcohols or adsorbed water, while the band at 3300 cm^{-1} is attributed to O-H stretching in carboxylic acids. The bands at 2960 and 2875 cm^{-1} correspond to the C-H asymmetric and symmetric stretching vibrations of CH_3 groups, respectively, of alkane chains. The band at 2510 cm^{-1} is related to the S-H stretching in thiols, the band 1730 cm^{-1} is due to the C=O stretching of aldehydes or esters, and the band at 1660 cm^{-1} is assigned to the C=C stretching of alkenes. The band at 1450 cm^{-1} is attributed to the bending vibrations of the

CH₂ groups, and the bands at the range 1065–1275 cm⁻¹ is attributed to the C-O stretching in esters, alcohols, or ethers. The band at 875 cm⁻¹ can be assigned to the C-H bending of aromatic trisubstituted compounds and to the CaCO₃, which is a typical additives in paints, being in agreement with the high Ca contents identified by EDS analysis [65–68]. NAS-3 is creosote-impregnated wood. The broad band at 3325 cm⁻¹ is attributed to the stretching mode of the O-H bonds existing in cellulose, the hemicellulose and lignin components of wood, and to traces of adsorbed water. The bands at 2925 cm⁻¹ and 2850 cm⁻¹ are related to the C-H asymmetric and symmetric stretching vibrations of CH₂ groups, respectively. The band at 1660 cm⁻¹ is attributed to the ring-conjugated C=O stretching of coniferyl or sinapyl aldehydes in lignin. The bands at 1600 cm⁻¹ and 1515 cm⁻¹ are attributed to the symmetric and asymmetric C=C aromatic skeletal vibrations of lignin. The strong band at 1025 cm⁻¹ is attributed to the C-O-C stretching of primary alcohol in cellulose and hemicellulose [69].

The results of the thermal stability analysis for each type of waste are presented in the form of TGA curves (thermogravimetric analysis) and their derivative DTG curves in Figure 4.

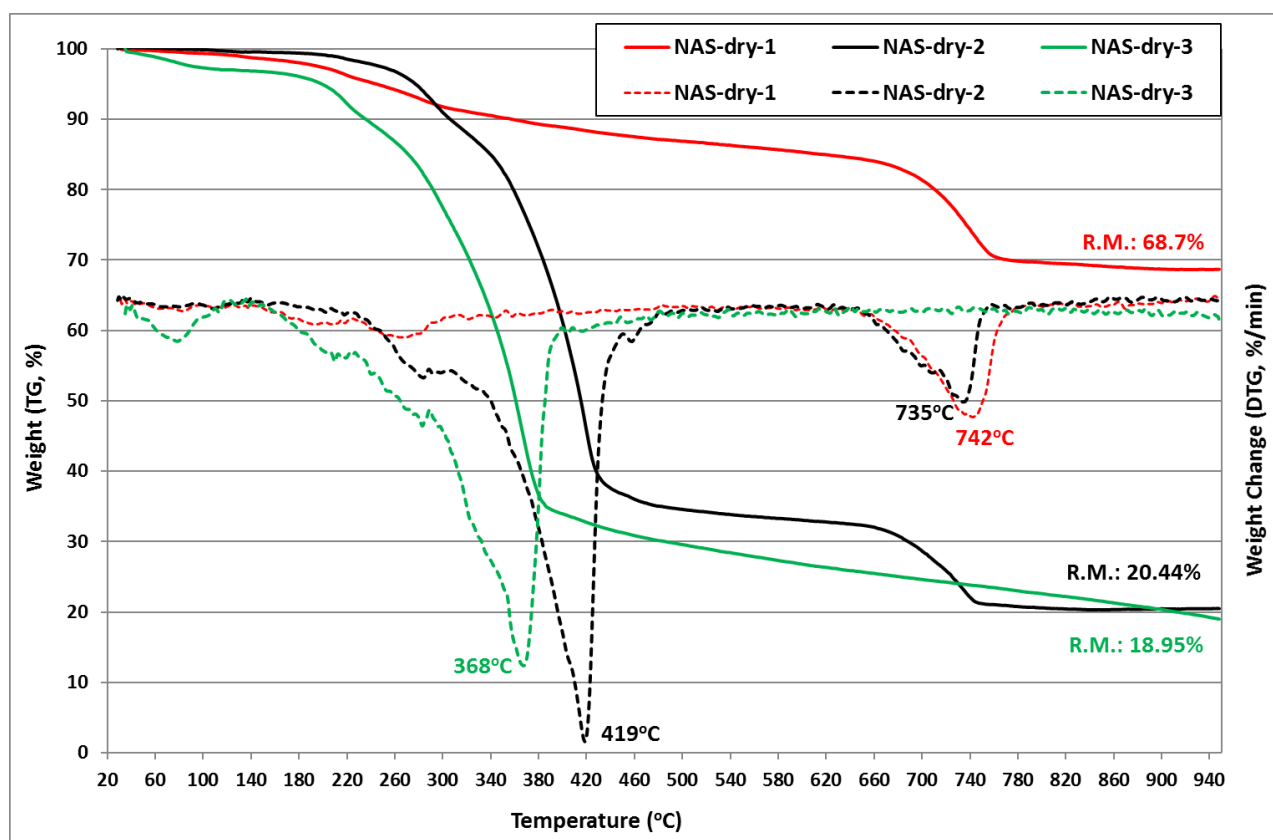


Figure 4. TGA/DTG curves of the three waste materials (in N₂ atmosphere).

The TGA curve of NAS-1 confirms the high ash content (~74 wt.%), because the weight loss up to 950 °C is approximately 33%. The difference of ~6% compared to ash determination is because the TGA measurements were taken under N₂ atmosphere, so the organic matter was not completely burned. A continuous gradual decrease of weight (~18%) from 150 to 600 °C was observed due to the evaporation and decomposition of relatively light hydrocarbons, while a sharper weight loss of ~12% was monitored between 650 and 770 °C due to the breakdown and desorption of the heavy aromatics of oil sludge. The TGA curve of NAS-2 shows a sharp and very intense weight loss in the range of 250 to 450 °C due to the breakdown of the hydrocarbons of the paint, mainly esters. It also shows a sharp but less pronounced weight decrease in the range of 650 to 750 °C, as in

the case of NAS-1, which is probably due to the existence and breakdown of aromatic compounds in the paint. The decomposition of CaCO_3 , contained in NAS-2, in the same temperature region may also contribute to the steep weight loss. The TGA curve of NAS-3 is typical of lignocellulosic biomass, with a sharp and very intense weight loss in the range of 200 to 400 °C due to the breakdown of the structural compounds of wood/biomass (hemicellulose, cellulose, and lignin). The thermal degradation and desorption of creosote may occur at higher temperatures, ca. > 500 °C, but a clear weight decrease cannot be identified, probably due to its relatively low content in the aged, impregnated wood waste.

3.2. Fast Pyrolysis of NAS Wastes on Py/GC-MS System

The non-catalytic and catalytic pyrolysis experiments of NAS wastes were performed at 600 °C. Representative Py/GC-MS spectra of NAS-1 pyrolysis experiment are shown in the Supplementary Material, Figure S3. The distribution of the product compounds among the various groups, i.e., mono-aromatics (AR); aliphatics (ALI); phenols (PH); acids (AC); esters (EST); alcohols (AL); ethers (ETH); aldehydes (ALD); ketones (KET); and polycyclic aromatic hydrocarbons, including naphthalenes (PAH's), sugars (SUG) nitrogen compounds (NIT), sulfur compounds (SUL), oxygenated aromatics (OxyAR), oxygenated phenols (OxyPH), and unidentified compounds (UN), derived both from the non-catalytic and catalytic pyrolysis of all NAS samples, is shown in Figure 5. In addition, full product lists for the three wastes are provided in Supplementary Materials, Tables S5–S8.

The pyrolysis oil produced from NAS-1 (oil sludge) by thermal (non-catalytic) pyrolysis experiments at 600 °C consists mainly of aliphatic hydrocarbons (~50%) and low/moderate percentages of mono-aromatic compounds (~18%), acids (~12%), alcohols (~6%), and esters (~4%) (Figure 5 and Supplementary Material, Table S5). In the catalytic pyrolysis experiment using the H-ZSM-5 zeolite as a catalyst, it is observed that the pyrolysis oil produced consisted mainly of mono-aromatic compounds (~63%), as well as less aliphatic compounds (~18%), polyaromatic compounds—mainly naphthalenes (~7.5%), esters (~3.2%), acids (~3%), and alcohols (~2%) (Figure 5 and Supplementary Material, Table S6). The comparison between the two different oils shows that, in catalytic pyrolysis, there is a significant tendency to reduce the formation of linear aliphatic hydrocarbons (mainly C9–C35 linear alkenes) resulting from the thermal pyrolysis/decomposition of the heavy hydrocarbons of the NAS-1, to form mainly BTX mono-aromatics (such as benzene, toluene, 1,3-dimethylbenzene, and relevant) and naphthalenes (such as naphthalene and 1 or 2-methyl-naphthalene), due to the strong Brønsted acidity and the particular microporosity of ZSM-5 (tubular pores with a diameter of approximately 5.5 Å), which make it extremely active for the formation of aromatic compounds [11,70].

From the experiments of thermal (non-catalytic) pyrolysis of paint residues (NAS-2), carried out at 600 °C using silica sand, it is observed that the pyrolysis oil consists mainly of esters (~62%) such as n-butyl methacrylate (~54%), which is indicative that this paint is based on acrylic esters, and alcohols, mainly sugar alcohols such as xylitol derivatives (~23%) (Figure 5 and Table 2). It also contains low percentages of aliphatic and oxy-aromatic compounds, at about ~7% and ~6%, respectively, as well as lower percentages of ketones (~1%) and nitrogen compounds (~1%). In contrast, during the catalytic pyrolysis of NAS-2 with the ZSM-5 catalyst, at the same temperature, the oil produced consisted of a high percentage of BTX mono-aromatic compounds (~73%) such as benzene, toluene, and 1,3-dimethylbenzene, and a few polyaromatic hydrocarbons—mainly naphthalenes (~11%), as well as some aliphatic hydrocarbons (~9%), esters (~4%), oxy-phenolic (~3%), and nitrates (~1%) (Figure 5 and Table 3). It can thus be suggested that the initially produced esters and alcohols can be further converted to mono-aromatics via dehydration, cracking, and aromatization reactions on ZSM-5 zeolite.

Table 2. Composition of bio-oil derived from non-catalytic fast pyrolysis of residual paint (NAS-2) in the Py/GC-MS system, at 600 °C (GC-MS peak area, %).

Compound	Group	%	Compound	Group	%
2-Hexen-1-ol, (Z)-	AL	0.15	Methyl stearate	EST	0.13
1,3,5-Hexatriene, (Z)-	ALI	0.60	Docosane	ALI	0.48
Propanoic acid, 2-methyl-, methyl ester	EST	0.39	Butyl 9-octadecenoate or 9-18:1	ALI	0.34
3-Pentanone	KET	0.06	Hexanedioic acid, bis(2-ethylhexyl) ester	EST	0.28
1-Deoxy-2,4-methylene-3,5-anhydro-d-xylitol	AL	21.76	Dodecanoic acid, undecyl ester	EST	0.23
Propanoic acid, 2,2-dimethyl-, methyl ester	EST	0.20	Butanedioic acid, 2,3-bis(benzoyloxy)-, [S-(R*,R*)]-	OxyAR	0.12
Oxazole, 4,5-dimethyl-	NIT	0.17	1,2-Benzenedicarboxylic acid, bis(8-methylnonyl) ester	EST	2.74
1-Decene	ALI	0.27	2(3H,4H)-Cyclopenta[b]furanone, 3a,6a-dihydro-	KET	0.21
1-Heptanol, 3-methyl-	AL	0.20	Oxetane, 3,3-dimethyl-	ALI	0.89
1,3-Hexanediol, 2-ethyl-	AL	0.12	1,5-Hexadiene, 2,5-dimethyl-	ALI	0.06
Propanoic acid, 2-methyl-, butyl ester	EST	0.45	1-Decene, 3,3,4-trimethyl-	ALI	0.06
Benzaldehyde	KET	0.32	2-Propenoic acid, butyl ester	EST	0.11
n-Butyl methacrylate	EST	54.25	2-Undecene, 2,5-dimethyl-	ALI	0.09
1,1-Cyclobutanedicarboxamide, 2-phenyl-N,N'-bis(1-phenylethyl)-	NIT	0.08	Propanoic acid, 2-methylpropyl ester	EST	0.57
Benzene, 1,2,3-trimethyl-	AR	0.11	cis-2-Allylpyrrolidin-5-ol	AL	0.13
Butyl 2-methylbutanoate	ALI	0.15	Acetic acid, octyl ester	EST	0.27
3-Dodecanone	ALI	0.09	3-Undecene, 6-methyl-, (E)-	ALI	0.11
CH ₂ =C(CH ₃)CH ₂ COOH	AC	0.20	2-Cyclopenten-1-one, 2,3-dimethyl-	KET	0.06
Acetophenone	KET	0.23	4-Undecene, 3-methyl-, (Z)-	ALI	0.16
Benzoic acid, methyl ester	EST	0.77	Benzonitrile	NIT	0.29
1-Propanone, 1-phenyl-	KET	0.18	5-Amino-1-benzoyl-1H-pyrazole-3,4-dicarbonitrile	NIT	0.14
1-Dodecene	ALI	3.14	n-Butyl tiglate	ALI	0.05
1,3-Dioxocane, 2-pentadecyl-	ALI	0.18	Butanoic acid, hexyl ester	EST	0.11
Phthalic anhydride	OxyAR	4.61	(S)-(+)-5-Methyl-1-heptanol	AL	0.13
1,2-Benzenedicarbonitrile	NIT	0.32	2-Decene, 2,4-dimethyl-	ALI	0.13
1(3H)-Isobenzofuranone	OxyAR	0.23	Cyclohexane, 1,2,4-trimethyl-	ALI	0.06
Butyl benzoate	OxyAR	0.65	Dimethyl cyclohexane-1,4-dicarboxylate (trans isomer)	ALI	0.04
.beta.-d-Lyxofuranoside, thio-nonyl-	SUL	0.11	2,4-Pentadienoic acid, 3,4-dimethyl-, isopropyl ester	EST	0.04
Benzophenone	KET	0.16	Propanoic acid, 3-hydroxy-2,2-dimethyl-, 3-hydroxy-2,2-dimethylpropyl ester	AC	0.08
2(1H)-Naphthalenone, 4a,5,6,7,8,8a-hexahydro-4a,8a-dimethyl-, cis-	KET	0.26	1,10-Dimethyl-2-methylene-trans-decalin	ALI	0.13
2-Hexadecene, 3,7,11,15-tetramethyl-, [R-[R*,R*-(E)]]-	ALI	0.22	n-Dodecylmethyl sulfide	SUL	0.06
Cyclo-(glycyl-l-leucyl)	NIT	0.25	1,2-Cyclohexanedicarboxylic acid, butyl isobutyl ester	EST	0.05
1-Isobutylpiperidine-4-carboxylic acid, (tetrahydrofuran-2-ylmethyl)amide	NIT	0.25	Benzoic acid, hex-3-yl ester	AC	0.05
9-Octadecenoic acid, methyl ester, (E)-	EST	0.13	Hexadecanoic acid, methyl ester	AC	0.09
			Octadecanoic acid, 12-hydroxy-, methyl ester	EST	0.13
			Butyl 9,12-octadecadienoate	ALI	0.05
			2-Cyclohexene-1,4-dione, 5,6-dibromo-2,6-dimethyl-, 1-oxime, o-benzoyl-	ALI	0.09

Table 3. Composition of bio-oil derived from catalytic fast pyrolysis (with ZSM-5 zeolite as catalysts) of residual paint (NAS-2) in the Py/GC-MS system, at 600 °C (GC-MS peak area, %).

Compound	Group	%	Compound	Group	%
Cyclopentene, 4-methyl-	ALI	1.07	Methyl methacrylate	EST	0.18
Benzene	AR	6.90	3-Methylenecyclohexene	ALI	0.17
Cyclopentane, 1,3-dimethyl-	ALI	0.67	2,4-Hexadiene, 3-methyl-	ALI	0.30
Cyclopentene, 4,4-dimethyl-	ALI	1.11	Cyclopentane, 1,2-dimethyl-3-methylene-, cis-	ALI	0.07
Cyclohexane, methyl-	ALI	0.15	.alpha.-Methylstyrene	AR	0.05
Cyclobutane, (1-methylethylidene)-	ALI	0.49	n-Butyl methacrylate	EST	0.57
Toluene	AR	14.26	Benzene, 1-ethenyl-3-methyl-	AR	0.11
Cyclopentene, 1,2,3-trimethyl-	ALI	0.39	Benzene, 2-propenyl-	AR	0.06
Ethylbenzene	AR	3.46	Benzene, 1,4-diethyl-	AR	0.09
Benzene, 1,3-dimethyl-	AR	20.38	Benzene, 1-methyl-4-propyl-	AR	0.15
o-Xylene	AR	5.16	2-Tolyloxirane	OxyAR	0.30
Benzene, propyl-	AR	0.31	5-Hexen-2-one, 5-methyl-3-methylene-	KET	0.04
Benzene, 1-ethyl-2-methyl-	AR	5.49	Benzene, 4-ethyl-1,2-dimethyl-	AR	0.29
Benzene, 1,2,4-trimethyl-	AR	7.29	Benzene, 1,2,3,4-tetramethyl-	AR	0.23
Benzonitrile	NIT	1.13	Benzene, 1,2,4,5-tetramethyl-	AR	0.08
Indane	AR	1.29	Benzene, 2-ethenyl-1,4-dimethyl-	AR	0.05
Indene	AR	0.96	Benzene, 1-methyl-4-(2-propenyl)-	AR	0.05
1-Phenyl-1-butene	PH	0.54	1H-Indene, 2,3-dihydro-5-methyl-	AR	0.74
2,4-Dimethylstyrene	AR	0.36	2-Methylindene	AR	0.35
1H-Indene, 2,3-dihydro-4-methyl-	AR	0.56	3-Phenylpropanoic anhydride	AR	0.08
1H-Indene, 3-methyl-	AR	1.41	1,4-Dihydronaphthalene	AR	0.05
1H-Indene, 1-methyl-	AR	0.37	2-Naphthalenol, 1,2-dihydro-, acetate	PAH	0.78
Naphthalene, 1,2,3,4-tetrahydro-	PAH	0.15	1H-Indene, 2,3-dihydro-1,6-dimethyl-	AR	0.08
Naphthalene	PAH	1.35	Phenol, 2,3-dimethyl-	PH	0.10
1H-Indene, 1,1-dimethyl-	AR	0.18	2-Ethyl-2,3-dihydro-1H-indene	AR	0.04
Naphthalene, 2-methyl-	PAH	3.22	1H-Indene, 1,3-dimethyl-	AR	0.58
Dodecane, 2,6,11-trimethyl-	ALI	0.21	Naphthalene, 1,2-dihydro-3-methyl-	PAH	0.14
Naphthalene, 1-ethyl-	PAH	0.45	Phenol, 2-ethyl-6-methyl-	PH	0.04
Naphthalene, 1,7-dimethyl-	PAH	0.59	Naphthalene, 6-ethyl-1,2,3,4-tetrahydro-	AR	0.04
Naphthalene, 2,3-dimethyl-	PAH	0.47	Naphthalene, 1-methyl-	PAH	0.19
Naphthalene, 1,5-dimethyl-	PAH	0.23	Phthalic anhydride	OxyAR	3.25
Hexadecane, 2,6,10,14-tetramethyl-	ALI	0.95	1,3-Dicyanobenzene	NIT	0.17
Eicosanoic acid	AC	0.18	1,2,3-Trimethylindene	AR	0.05
Pentadecane, 2,6,10-trimethyl-	ALI	0.35	1H-Indene, 1,1,3-trimethyl-	AR	0.06
Pentadecane, 2,6,10,14-tetramethyl-	ALI	0.63	Naphthalene, 2,6-dimethyl-	PAH	1.03
Dotriacontyl heptafluorobutyrate	ALI	0.49	1H-Isoindole-1,3(2H)-dione, 2-methyl-	AL	0.16
Tetrapentacontane, 1,54-dibromo-	ALI	0.07	1H-Isoindole-1,3(2H)-dione, 2-(hydroxymethyl)-	AR	0.22
n-Tetracosanol-1	AL	0.15			
Oxalic acid, allyl octadecyl ester	EST	0.16	Naphthalene, 2-(1-methylethyl)-	PAH	0.13
Heptafluorobutyric acid, n-tetradecyl ester	EST	0.41	Naphthalene, 1,4,6-trimethyl-	PAH	0.07
2-Octadecyl-propane-1,3-diol	AL	1.48	Naphthalene, 1,6,7-trimethyl-	PAH	0.06
Sulfurous acid, octadecyl 2-propyl ester	EST	2.75	Anthracene	PAH	0.07
1,4-Hexadiene, (Z)-	ALI	0.22	Phenanthrene, 2-methyl-	PAH	0.07
Cyclopentene, 1,5-dimethyl-	ALI	0.23	Palmitoleic acid	AC	0.04

The pyrolysis oil produced by the thermal (non-catalytic) pyrolysis experiments of wood impregnated with creosote oil (NAS-3), at 600 °C, consists mainly of polyaromatic hydrocarbons—PAHs (~62%)—such as pyrene, benz[a]anthracene, and fluoranthene, and oxy-phenols (~19%) such as creosol, trans-isoeugenol, and 2-methoxy-phenol, with a smaller concentration of furans (~3%), ketones (~3%), nitrogen compounds (~4%), sulfur

compounds (~3%), mono-aromatic compounds (~2%), phenols (~1%), and oxy-aromatic compounds (~1%) (Figure 5 and Supplementary Material, Table S7). PAHs may be derived from the thermal decomposition of the creosote used as preservative of the wastes studied here, which seems to be related to coal-tar creosote rather than wood-tar creosote derived from wood (i.e., beech-tar creosote). This is in line with the relatively high sulfur levels measured by the elemental analysis of NAS-3 (discussed above). Additionally, the pyrolysis oil contains 3% sulfur compounds. The identified oxy-phenols originated from the thermal decomposition of lignin in the wood, but may also come from wood-tar if a mixed coal/wood tar creosote was used. In contrast, during the catalytic cracking of NAS-3 using ZSM-5 zeolite, at the same temperature, the oil produced consists mainly of naphthalenes (~9%) and larger PAHs (~40%), mono-aromatic compounds (~39%), and a smaller percentages of other compounds, such as furans (~4%), oxy-phenolic compounds (~2%), aliphatic compounds (~2%), sulfur compounds (~1%), phenols (~1%), and ketones (~1%) (Figure 5 and Supplementary Material, Table S8). The composition of the catalytic pyrolysis oil of the creosote-impregnated wood can be rationalized via two main reaction pathways. One is the known ability of ZSM-5 zeolite catalyst to convert the initially formed (via thermal degradation of lignin in the wood) oxy-phenols to BTX mono-aromatics via decarbonylation, decarboxylation, dehydration/dehydroxylation, cracking, dealkylation, aromatization, and (trans)alkylation and disproportionation reactions [11,15]. These mono-aromatics can undergo further condensation reactions on ZSM-5 towards PAHs, mainly naphthalenes [11]. The second path involves the partial cracking of the recalcitrant PAHs (with >2 aromatic rings) that may occur on the strongly acidic ZSM-5 towards smaller naphthalenes and mono-aromatics. The activity of ZSM-5 in the cracking of PAHs is also restricted by its small pore size (~0.55 nm).

3.3. Fast Pyrolysis of NAS Wastes on Bench-Scale Fixed-Bed Reactor

The fast pyrolysis of the three solid wastes was also studied on a fixed-bed pyrolysis reactor in order to determine the product yields, i.e., pyrolysis oil, non-condensable gases, and solids (as described in the experimental section). Photographs of chars and pyrolysis oils obtained are shown in Figure 6.

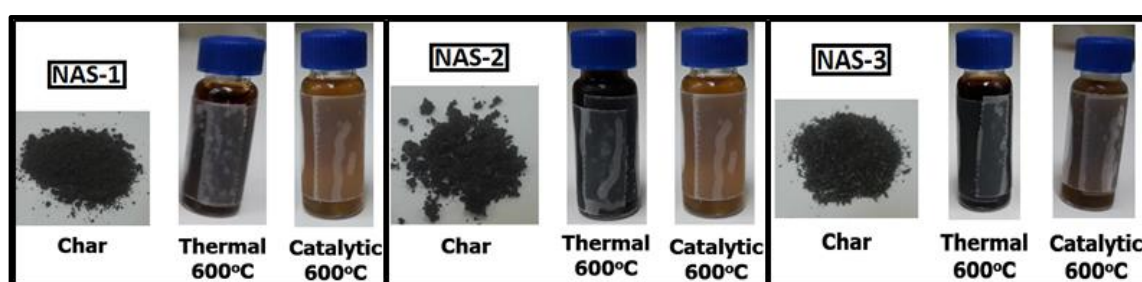


Figure 6. Char and pyrolysis oils obtained from the three solid organic wastes.

3.3.1. Petroleum Containing Sludge (NAS-1) Pyrolysis Results

The product yields obtained from the thermal (non-catalytic) and catalytic pyrolysis of the petroleum containing sludges are presented in Table 4. The thermal pyrolysis oil obtained from this waste material accounted only for 15.8 wt.% (based on dry feed), consisting of 10.3 wt.% organic compounds and 5.5 wt.% water. The non-condensable gases (7.9 wt.% on feed) consisted mainly of CO₂, and smaller amounts of CO and methane. On the other hand, the recovered solids were remarkably high, up to 75.1 wt.%, which consisted mainly of inorganics/ash. The measured ash of the dry waste feed was found to be ~74 wt.% (Supplementary Material, Table S1); thus, a low amount of ~1 wt.% on feed may account for the char originating from the petroleum fraction. The pyrolysis oil (12.6 wt.%) obtained by the use of ZSM-5(40) zeolite catalyst has a very low organic content and contains mainly water due to deoxygenation/dehydration reaction of impurities of oxygenated compounds and fatty acids. The strongly acidic ZSM-5 zeolite induces cracking

reactions of the paraffinic molecules formed via the initial thermal decomposition of the heavy oil waste towards small alkenes, which can be further converted to BTX mono-aromatics via oligomerization/cyclization and dehydrogenation reactions on the Brønsted acid sites of ZSM-5, as discussed above for the Py/GC-MS catalytic pyrolysis results [11,71]. This mechanism is also supported by the increased content of ethylene and propylene in the gases, both being typical hydrocarbon catalytic cracking products, and can serve as a basis for the aromatization reactions. In addition to the total gases increase using ZSM-5 (~10 wt.%), the solids were also slightly higher (76.2 wt.%), due to the formation of a small amount of reaction-coke on the catalyst (1.1 wt.%) (Table 4).

Table 4. Product yields in thermal and catalytic fast pyrolysis of petroleum containing sludge (NAS-1), at 600 °C, obtained on fixed-bed reactor (C/F mass ratio = 1).

Petroleum Sludges Pyrolysis	Thermal	ZSM-5 (40)
Total Liquids (wt.%)	15.8	12.6
Organic oil (wt.%)	10.3	2.3
Water (wt.%)	5.5	10.3
Total Gases (wt.%)	7.9	10.0
H ₂ (wt.%)	0.14	0.11
CH ₄ (wt.%)	0.90	0.55
Ethylene (wt.%)	-	1.67
Propylene (wt.%)	-	2.70
C ₄ ⁺ (wt.%)	-	1.23
CO ₂ (wt.%)	5.97	3.01
CO (wt.%)	0.86	0.74
Total Solids (Ash + Char + Coke on catalyst) (wt.%)	75.1	76.2
Coke on catalyst (difference of Ash + char + coke minus Ash + char from the thermal pyrolysis experiment) (wt.%)	-	1.1
Total Mass Balance (wt.%)	98.8	98.8

3.3.2. Residual Paint on Metal Containers (NAS-2) Pyrolysis Results

The product yields obtained from the thermal and catalytic pyrolysis of the residual paint on scrap metals (NAS-2) are presented in Table 5. The thermal pyrolysis oil yield was 35 wt.% and consisted mainly of organics (24 wt.%), i.e., esters and sugar alcohols, as discussed above based on the Py/GC-MS results. The gases were 19.2 wt.%, comprising mainly of propylene (~8.4 wt.%) and C₄+ hydrocarbons, as well as some CO, ethane, and propane. Propylene represents 43% of the pyrolysis gases, thus making this type of organic waste a potentially valuable source of this high-added-value building block in the polymer industry. The solids yield was 36.9 wt.%, with 6.9 wt.% accounting for the formed char because the ash of this waste is ~30 wt.% (Supplementary Material, Table S1). The use of ZSM-5 zeolite led to less organics due to their conversion to gases (26.3 wt.%, 7.1 wt.% more than the thermal pyrolysis gases) and coke (1.4 wt.% on feed). The water content of the pyrolysis oil was increased due to the deoxygenation/dehydration reactions of the esters and alcohols during the pyrolysis process. The gases consisted mainly of ethane, propane, and C₄+ hydrocarbons as well as CO, CO₂, methane, ethylene, and propylene. Propylene, despite being a catalytic pyrolysis product, is lower with ZSM-5 compared to the thermal pyrolysis gases, as it was converted to BTX mono-aromatics, as discussed above (Figure 5 and Table 3).

3.3.3. Creosote-Treated Wood Waste (NAS-3) Pyrolysis Results

The product yields obtained from the thermal and catalytic pyrolysis of the creosote-treated wood waste (NAS-3) are shown in Table 6. The thermal (non-catalytic) pyrolysis of this waste material provides a substantially higher oil yield, compared to the previous wastes, which is 46.9% wt. of the initial feed and consists of 31.6 wt.% organic compounds and 15.3 wt.% water. The main compounds of the pyrolysis oil were PAHs (pyrene, benz[a]anthracene, and fluoranthene) originating from the decomposition of creosote and oxy-phenols (creosol, trans-iso Eugenol, and 2-methoxy-phenol) originating from the degra-

duction of lignin in the wood, as is also discussed in the previous section [15,16,19,20,72]. The total gases were ~14.8 wt.% (based on feed) and consisted mainly of CO₂ and CO with smaller amounts of methane, this composition being typical for the fast pyrolysis of various types of lignocellulosic biomass [15,19,20,73]. The solids (36.0 wt.%) are mainly attributed to the char produced from the pyrolysis of the wood as well as to some contribution from coke originating from the thermal pyrolysis of the creosote.

Table 5. Product yields in thermal and catalytic fast pyrolysis of residual paints, at 600 °C, obtained on fixed-bed reactor (C/F mass ratio = 1).

Residual Paints Pyrolysis	Thermal	ZSM-5 (40)
Total Liquids (wt.%)	35.0	32.4
Organic oil (wt.%)	24.0	16.5
Water (wt.%)	11.0	15.9
Total Gases (wt.%)	19.2	26.3
H ₂ (wt.%)	0.07	0.07
CH ₄ (wt.%)	-	0.21
Ethane (wt.%)	0.32	4.27
Ethylene (wt.%)	-	0.47
Propane (wt.%)	0.83	7.30
Propylene (wt.%)	8.39	3.55
C ₄ ⁺ (wt.%)	7.05	4.27
CO ₂ (wt.%)	-	0.21
CO (wt.%)	1.64	5.39
Total Solids (Char + Coke on catalyst) (wt.%)	36.9	38.3
Coke on catalyst (difference of char + coke minus char from the thermal experiment) (wt.%)	-	1.4
Total Mass Balance (wt.%)	91.1	97.1

Table 6. Product yields in thermal and catalytic fast pyrolysis of creosote-treated wood waste (NAS-3), at 600 °C, obtained on fixed-bed reactor (Catalyst/feed mass ratio = 1).

Creosote-Treated Wood Waste	Thermal	ZSM-5 (40)
Total Liquids (wt.%)	46.9	41.9
Organic oil (wt.%)	31.6	17.3
Water (wt.%)	15.3	24.6
Total Gases (wt.%)	14.7	17.3
H ₂ (wt.%)	0.1	0.03
CH ₄ (wt.%)	1.44	0.79
Ethane (wt.%)	-	-
Ethylene (wt.%)	-	1.4
Propane (wt.%)	-	-
Propylene (wt.%)	0.14	1.07
C ₄ ⁺ (wt.%)	-	0.11
CO ₂ (wt.%)	8.29	6.18
CO (wt.%)	4.77	7.69
Total Solids (Char + Coke on catalyst) (wt.%)	36.0	38.4
Coke on catalyst (difference of char + coke minus char from the thermal experiment) (wt.%)	-	2.4
Total Mass Balance (wt.%)	97.6	97.6

The use of ZSM-5 zeolite induced similar effects to the previous wastes, by converting the organics towards gases (17.3 wt.%) as well as some reaction coke (2.4 wt.%), leading to a decrease of pyrolysis oil yield (41.9 wt.%), with almost half organics (17.3 wt.%) and much higher water content (24.6 wt.%) compared to the thermal pyrolysis oil. As discussed above, the catalytic pyrolysis oil contained relatively less larger PAHs, and substantially more BTX mono-aromatics and naphthalenes, as a result of the partial cracking of the resistant PAHs and of the conversion of the alkoxy-phenolics (originating from the thermal pyrolysis of wood) to aromatics via decarbonylation, decarboxylation, dehydration/dehydroxylation, cracking, dealkylation, aromatization and (trans)alkylation, and disproportionation reactions [11,15]. The catalytic pyrolysis gases consisted again mainly of CO and CO₂, with increased amounts of ethylene and propylene being typical cracking products on ZSM-5.

The solids were also slightly increased from 36.0 wt.% to 36.8 wt.% due to the formation of reaction coke.

4. Conclusions

In this study, different hazardous organic waste materials were tested as fast pyrolysis feeds in order to investigate the potential of a possible industrial management and valorization process. As expected, the pyrolysis products were dependent on the nature and composition of the feed waste, but overall, it was shown that the fast pyrolysis process can be utilized and can provide a wide range of valuable products.

Petroleum sludges contain high amounts of inorganics/ash (sediments, dust, soil, rust, etc.) leaving a low (ca. < 25 wt.% for the waste of this study) organic fraction for recycling and valorization. The application of catalytic fast pyrolysis using acidic ZSM-5 zeolite (or the in situ catalytic upgrading of thermal pyrolysis vapors) is highly recommended for this waste, as the initially produced high MW hydrocarbons can be converted to a pyrolysis oil enriched with added-value BTX mono-aromatics.

On the other hand, the thermal pyrolysis of the residual paints recovered from waste containers affords a pyrolysis oil enriched in acrylic esters, such as n-butyl methacrylate, which is considered as a valuable monomer for the polymer and paint industry. Furthermore, the thermal pyrolysis gases contain substantial amounts of propylene (ca. ~8.4 wt.% on feed), which is also a valuable monomer for making polypropylene and other chemicals. Still, the use of ZSM-5 as a catalyst in the catalytic pyrolysis of residual paints resulted in a highly enriched BTX aromatics oil, in addition to appreciable amounts of propylene.

The thermal pyrolysis of creosote-treated wood waste provided a pyrolysis oil that contained mainly PAHs with more 3–5 aromatic rings from the decomposition of creosote as well as some oxy-phenols from the decomposition of lignin in the wood. The use of ZSM-5 zeolite catalyst managed to partially reduce the concentration of large PAHs towards smaller naphthalenes via cracking and at the same time to produce BTX mono-aromatics via deoxygenation and aromatization reactions of oxy-phenols.

Although the catalytic upgrading with ZSM-5 zeolite may offer pyrolysis oils enriched in high-added-value BTX aromatics and at the same time deoxygenate the oils (thus increasing their heating value), it also leads to lower organic oil yields and limited formation reaction-coke (on the catalyst). Overall, fast pyrolysis, with or without the use of an acidic catalyst, exhibits a high potential in the recycling and valorization of the studied wastes towards chemicals and fuels, in addition to the recovered (bio)char, which may be also utilized in various applications.

Supplementary Materials: The following supporting information can be downloaded at: <https://www.mdpi.com/article/10.3390/suschem3010007/s1>, Figure S1: Schematic representation of the Py/GC-MS system, Figure S2: Schematic representation of bench-scale fixed-bed reactor for fast pyrolysis of solid wastes, Figure S3: Representative Py/GC-MS spectra of the non-catalytic (thermal) and catalytic fast pyrolysis of NAS-1 at 600 °C, Table S1: Waste materials physicochemical properties, Table S2: Composition of the ash of the three waste feeds, Table S3: Elemental analysis of waste materials (normalized values⁽¹⁾), Table S4: FT-IR bands identification for the solid waste materials, Table S5: Composition of bio-oil derived from non-catalytic fast pyrolysis of petroleum sludge (NAS-1) in the Py/GC-MS system, at 600 °C (GC-MS peak area, %), Table S6: Composition of bio-oil derived from catalytic fast pyrolysis (with ZSM-5 zeolite as catalysts) of petroleum sludge (NAS-1) in the Py/GC-MS system, at 600 °C (GC-MS peak area, %), Table S7: Composition of bio-oil derived from non-catalytic fast pyrolysis of creosote-impregnated wood (NAS-3) in the Py/GC-MS system, at 600 °C (GC-MS peak area, %), Table S8: Composition of bio-oil derived from catalytic fast pyrolysis (with ZSM-5 zeolite as catalysts) of creosote-impregnated wood (NAS-3) in the Py/GC-MS system, at 600 °C (GC-MS peak area, %).

Author Contributions: Conceptualization, K.C.R., I.D.C., A.I.Z. and K.S.T.; methodology, K.C.R., I.D.C., A.I.Z. and K.S.T.; validation, K.C.R., I.D.C., E.T., G.P., A.I.Z. and K.S.T.; formal analysis, K.C.R., I.D.C., E.T., G.P., A.I.Z. and K.S.T.; investigation, K.C.R., I.D.C. and K.S.T.; resources, A.I.Z. and K.S.T.; data curation, K.C.R., I.D.C., A.I.Z. and K.S.T.; writing—original draft preparation, K.C.R., I.D.C.,

E.T., G.P., A.I.Z. and K.S.T.; writing—review and editing, K.C.R., I.D.C., E.T., G.P., A.I.Z. and K.S.T.; visualization, K.C.R., I.D.C., A.I.Z. and K.S.T.; supervision, A.I.Z. and K.S.T.; project administration, A.I.Z. and K.S.T.; funding acquisition, A.I.Z. and K.S.T. All authors have read and agreed to the published version of the manuscript.

Funding: The authors wish to acknowledge co-funding of this research by the European Union-European Regional Development Fund; the Greek Ministry of Economy and Development; and the Greek Ministry of Education, Research, and Religious Affairs/GGET—EYDE-ETAK through program EPANEK 2014–2020/Action “RESEARCH—CREATE—INNOVATE” (project T1EDK-04491).

Data Availability Statement: The datasets generated during and/or analyzed during the current study are available from the corresponding author on reasonable request.

Conflicts of Interest: The authors declare no conflict of interest.

References

1. European Parliament Council. *Council Directive 2008/98/EC of 19 November 2008 on Waste and Repealing Certain Directives*; European Union: Luxembourg, 2008; p. 02008L0098.
2. Lombardi, L.; Carnevale, E.; Corti, A. A review of technologies and performances of thermal treatment systems for energy recovery from waste. *Waste Manag.* **2015**, *37*, 26–44. [[CrossRef](#)] [[PubMed](#)]
3. Munir, M.T.; Mohaddespour, A.; Nasr, A.T.; Carter, S. Municipal solid waste-to-energy processing for a circular economy in New Zealand. *Renew. Sustain. Energy Rev.* **2021**, *145*, 111080. [[CrossRef](#)]
4. Block, C.; Van Caneghem, J.; Van Brecht, A.; Wauters, G.; Vandecasteele, C. Incineration of Hazardous Waste: A Sustainable Process. *Waste Biomass Valorization* **2015**, *6*, 137–145. [[CrossRef](#)]
5. National Research Council. *Opportunities and Obstacles in Large-Scale Biomass Utilization: The Role of the Chemical Sciences and Engineering Communities: A Workshop Summary*; The National Academies Press: Washington, DC, USA, 2012; p. 60.
6. Bridgwater, A.V. Review of fast pyrolysis of biomass and product upgrading. *Biomass Bioenergy* **2012**, *38*, 68–94. [[CrossRef](#)]
7. Sharifzadeh, M.; Sadeqzadeh, M.; Guo, M.; Borhani, T.N.; Murthy Konda, N.V.S.N.; Garcia, M.C.; Wang, L.; Hallett, J.; Shah, N. The multi-scale challenges of biomass fast pyrolysis and bio-oil upgrading: Review of the state of art and future research directions. *Prog. Energy Combust. Sci.* **2019**, *71*, 1–80. [[CrossRef](#)]
8. Oasmaa, A.; Lehto, J.; Solantausta, Y.; Kallio, S. Historical Review on VTT Fast Pyrolysis Bio-oil Production and Upgrading. *Energy Fuels* **2021**, *35*, 5683–5695. [[CrossRef](#)]
9. Sorunmu, Y.; Billen, P.; Spataro, S. A review of thermochemical upgrading of pyrolysis bio-oil: Techno-economic analysis, life cycle assessment, and technology readiness. *GCB Bioenergy* **2020**, *12*, 4–18. [[CrossRef](#)]
10. Charisteidis, I.; Lazaridis, P.; Fotopoulos, A.; Pachatouridou, E.; Matsakas, L.; Rova, U.; Christakopoulos, P.; Triantafyllidis, K. Catalytic Fast Pyrolysis of Lignin Isolated by Hybrid Organosolv—Steam Explosion Pretreatment of Hardwood and Softwood Biomass for the Production of Phenolics and Aromatics. *Catalysts* **2019**, *9*, 935. [[CrossRef](#)]
11. Lazaridis, P.A.; Fotopoulos, A.P.; Karakoulia, S.A.; Triantafyllidis, K.S. Catalytic Fast Pyrolysis of Kraft Lignin With Conventional, Mesoporous and Nanosized ZSM-5 Zeolite for the Production of Alkyl-Phenols and Aromatics. *Front. Chem.* **2018**, *6*, 295. [[CrossRef](#)]
12. Kalogiannis, K.G.; Matsakas, L.; Lappas, A.A.; Rova, U.; Christakopoulos, P. Aromatics from Beechwood Organosolv Lignin through Thermal and Catalytic Pyrolysis. *Energies* **2019**, *12*, 1606. [[CrossRef](#)]
13. Kalogiannis, K.G.; Stefanidis, S.D.; Michailof, C.M.; Lappas, A.A.; Sjöholm, E. Pyrolysis of lignin with 2DGC quantification of lignin oil: Effect of lignin type, process temperature and ZSM-5 in situ upgrading. *J. Anal. Appl. Pyrolysis* **2015**, *115*, 410–418. [[CrossRef](#)]
14. Mondal, A.K.; Qin, C.; Ragauskas, A.J.; Ni, Y.; Huang, F. Preparation and Characterization of Various Kraft Lignins and Impact on Their Pyrolysis Behaviors. *Ind. Eng. Chem. Res.* **2020**, *59*, 3310–3320. [[CrossRef](#)]
15. Margellou, A.G.; Lazaridis, P.A.; Charisteidis, I.D.; Nitsos, C.K.; Pappa, C.P.; Fotopoulos, A.P.; Van den Bosch, S.; Sels, B.F.; Triantafyllidis, K.S. Catalytic fast pyrolysis of beech wood lignin isolated by different biomass (pre)treatment processes: Organosolv, hydrothermal and enzymatic hydrolysis. *Appl. Catal. A Gen.* **2021**, *623*, 118298. [[CrossRef](#)]
16. Liu, C.; Wang, H.; Karim, A.M.; Sun, J.; Wang, Y. Catalytic fast pyrolysis of lignocellulosic biomass. *Chem. Soc. Rev.* **2014**, *43*, 7594–7623. [[CrossRef](#)] [[PubMed](#)]
17. Imran, A.; Bramer, E.A.; Seshan, K.; Brem, G. An overview of catalysts in biomass pyrolysis for production of biofuels. *J. Biofuel Res. J.* **2018**, *5*, 872–885. [[CrossRef](#)]
18. Iliopoulou, E.F.; Lazaridis, P.A.; Triantafyllidis, K.S. Nanocatalysis in the Fast Pyrolysis of Lignocellulosic Biomass. In *Nanotechnology in Catalysis*; Springer: Berlin/Heidelberg, Germany, 2017; pp. 655–714.
19. Iliopoulou, E.F.; Triantafyllidis, K.S.; Lappas, A.A. Overview of catalytic upgrading of biomass pyrolysis vapors toward the production of fuels and high-value chemicals. *WIREs Energy Environ.* **2019**, *8*, e322. [[CrossRef](#)]

20. Triantafyllidis, K.S.; Stefanidis, S.D.; Karakoulia, S.A.; Pineda, A.; Margellou, A.; Kalogiannis, K.G.; Iliopoulou, E.F.; Lappas, A.A. Lappas. 5. State-of-the-art in biomass fast pyrolysis using acidic catalysts: Direct comparison between microporous zeolites, mesoporous aluminosilicates and hierarchical zeolites. In *Biomass and Biowaste*; Balu, A.M., Nuñez, A.G., Eds.; De Gruyter: Berlin, Germany, 2020; pp. 113–144.
21. Rahman, M.M.; Liu, R.; Cai, J. Catalytic fast pyrolysis of biomass over zeolites for high quality bio-oil—A review. *Fuel Processing Technol.* **2018**, *180*, 32–46. [[CrossRef](#)]
22. Kim, J.-Y.; Moon, J.; Lee, J.H.; Jin, X.; Choi, J.W. Conversion of phenol intermediates into aromatic hydrocarbons over various zeolites during lignin pyrolysis. *Fuel* **2020**, *279*, 118484. [[CrossRef](#)]
23. Li, J.; Li, X.; Zhou, G.; Wang, W.; Wang, C.; Komarneni, S.; Wang, Y. Catalytic fast pyrolysis of biomass with mesoporous ZSM-5 zeolites prepared by desilication with NaOH solutions. *Appl. Catal. A Gen.* **2014**, *470*, 115–122. [[CrossRef](#)]
24. Carlson, T.R.; Cheng, Y.-T.; Jae, J.; Huber, G.W. Production of green aromatics and olefins by catalytic fast pyrolysis of wood sawdust. *Energy Environ. Sci.* **2011**, *4*, 145–161. [[CrossRef](#)]
25. Foster, A.J.; Jae, J.; Cheng, Y.-T.; Huber, G.W.; Lobo, R.F. Optimizing the aromatic yield and distribution from catalytic fast pyrolysis of biomass over ZSM-5. *Appl. Catal. A Gen.* **2012**, *423–424*, 154–161. [[CrossRef](#)]
26. Carlson, T.R.; Vispute, T.P.; Huber, G.W. Green Gasoline by Catalytic Fast Pyrolysis of Solid Biomass Derived Compounds. *ChemSusChem* **2008**, *1*, 397–400. [[CrossRef](#)] [[PubMed](#)]
27. Gayubo, A.G.; Aguayo, A.T.; Atutxa, A.; Aguado, R.; Olazar, M.; Bilbao, J. Transformation of Oxygenate Components of Biomass Pyrolysis Oil on a HZSM-5 Zeolite. II. Aldehydes, Ketones, and Acids. *Ind. Eng. Chem. Res.* **2004**, *43*, 2619–2626. [[CrossRef](#)]
28. Mihalcik, D.J.; Mullen, C.A.; Boateng, A.A. Screening acidic zeolites for catalytic fast pyrolysis of biomass and its components. *J. Anal. Appl. Pyrolysis* **2011**, *92*, 224–232. [[CrossRef](#)]
29. Gamliel, D.P.; Cho, H.J.; Fan, W.; Valla, J.A. On the effectiveness of tailored mesoporous MFI zeolites for biomass catalytic fast pyrolysis. *Appl. Catal. A Gen.* **2016**, *522*, 109–119. [[CrossRef](#)]
30. Zheng, A.; Zhao, Z.; Chang, S.; Huang, Z.; Wu, H.; Wang, X.; He, F.; Li, H. Effect of crystal size of ZSM-5 on the aromatic yield and selectivity from catalytic fast pyrolysis of biomass. *J. Mol. Catal. A Chem.* **2014**, *383–384*, 23–30. [[CrossRef](#)]
31. Wang, K.; Kim, K.H.; Brown, R.C. Catalytic pyrolysis of individual components of lignocellulosic biomass. *Green Chem.* **2014**, *16*, 727–735. [[CrossRef](#)]
32. Hu, G.J.; Li, J.B.; Zeng, G.M. Recent development in the treatment of oily sludge from petroleum industry: A review. *J. Hazard. Mater.* **2013**, *261*, 470–490. [[CrossRef](#)]
33. Chen, H.S.; Zhang, Q.M.; Yang, Z.J.; Liu, Y.S. Research on Treatment of Oily Sludge from the Tank Bottom by Ball Milling Combined with Ozone-Catalyzed Oxidation. *ACS Omega* **2020**, *5*, 12259–12269. [[CrossRef](#)]
34. Badrul, I. Petroleum Sludge, its Treatment and Disposal: A Review. *Int. J. Chem. Sci.* **2015**, *13*, 1584–1602.
35. Al-Futaisi, A.; Jamrah, A.; Yaghi, B.; Taha, R. Assessment of alternative management techniques of tank bottom petroleum sludge in Oman. *J. Hazard. Mater.* **2007**, *141*, 557–564. [[CrossRef](#)] [[PubMed](#)]
36. Li, C.-T.; Lee, W.-J.; Mi, H.-H.; Su, C.-C. PAH emission from the incineration of waste oily sludge and PE plastic mixtures. *Sci. Total Environ.* **1995**, *170*, 171–183. [[CrossRef](#)]
37. Liu, J.; Jiang, X.; Zhou, L.; Han, X.; Cui, Z. Pyrolysis treatment of oil sludge and model-free kinetics analysis. *J. Hazard. Mater.* **2009**, *161*, 1208–1215. [[CrossRef](#)] [[PubMed](#)]
38. Liu, J.; Jiang, X.; Han, X. Devolatilization of oil sludge in a lab-scale bubbling fluidized bed. *J. Hazard. Mater.* **2011**, *185*, 1205–1213. [[CrossRef](#)]
39. Chang, C.-Y.; Shie, J.-L.; Lin, J.-P.; Wu, C.-H.; Lee, D.-J.; Chang, C.-F. Major Products Obtained from the Pyrolysis of Oil Sludge. *Energy Fuels* **2000**, *14*, 1176–1183. [[CrossRef](#)]
40. Wang, Z.; Gong, Z.; Wang, Z.; Li, X.; Chu, Z. Application and development of pyrolysis technology in petroleum oily sludge treatment. *Environ. Eng. Res.* **2021**, *26*, 190460. [[CrossRef](#)]
41. Lin, B.; Huang, Q.; Ali, M.; Wang, F.; Chi, Y.; Yan, J. Continuous catalytic pyrolysis of oily sludge using U-shape reactor for producing saturates-enriched light oil. *Proc. Combust. Inst.* **2019**, *37*, 3101–3108. [[CrossRef](#)]
42. Lenka, M.; Peter, E. *End-of-Waste Criteria for Iron and Steel Scrap: Technical Proposals*; European Commission. Joint Research Centre. Institute for Prospective Technological Studies; Publications Office: Luxembourg, 2010.
43. Nitsos, C.K.; Choli-Papadopoulou, T.; Matis, K.A.; Triantafyllidis, K.S. Optimization of Hydrothermal Pretreatment of Hardwood and Softwood Lignocellulosic Residues for Selective Hemicellulose Recovery and Improved Cellulose Enzymatic Hydrolysis. *ACS Sustain. Chem. Eng.* **2016**, *4*, 4529–4544. [[CrossRef](#)]
44. Tian, J.; Ni, F.J.; Chen, M. Application of pyrolysis in dealing with end-of-life vehicular products: A case study on car bumpers. *J. Clean. Prod.* **2015**, *108*, 1177–1183. [[CrossRef](#)]
45. Santos, J.I.; Martín-Sampedro, R.; Fillat, Ú.; Oliva, J.M.; Negro, M.J.; Ballesteros, M.; Eugenio, M.E.; Ibarra, D. Evaluating Lignin-Rich Residues from Biochemical Ethanol Production of Wheat Straw and Olive Tree Pruning by FTIR and 2D-NMR. *Int. J. Polym. Sci.* **2015**, *2015*, 314891. [[CrossRef](#)]
46. Thierfelder, T.; Sandstrom, E. The creosote content of used railway cross-ties as compared with European stipulations for hazardous waste. *Sci. Total Environ.* **2008**, *402*, 106–112. [[CrossRef](#)]
47. Hutzinger, O. *The Handbook of Environmental Chemistry. Volume 3 Pt. D: Anthropogenic Compounds*; Addison, R.F., Hutzinger, O., Eds.; Springer: Berlin, Germany, 1986.

48. Jung, S.H.; Koo, W.M.; Kim, J.S. Fast pyrolysis of creosote treated wood ties in a fluidized bed reactor and analytical characterization of product fractions. *Energy* **2013**, *53*, 33–39. [CrossRef]
49. Hoang Pham, L.K.; Vi Tran, T.T.; Kongparakul, S.; Reubroycharoen, P.; Ding, M.; Guan, G.; Vo, D.-V.N.; Jaiyong, P.; Youngvises, N.; Samart, C. Data-driven prediction of biomass pyrolysis pathways toward phenolic and aromatic products. *J. Environ. Chem. Eng.* **2021**, *9*, 104836. [CrossRef]
50. Maksimuk, Y.; Antonava, Z.; Krouk, V.; Korsakova, A.; Kursevich, V. Prediction of higher heating value based on elemental composition for lignin and other fuels. *Fuel* **2020**, *263*, 116727. [CrossRef]
51. Annamalai, K.; Sweeten, J.M.; Ramalingam, S.C. Technical Notes: Estimation of Gross Heating Values of Biomass Fuels. *Trans. ASAE* **1987**, *30*, 1205–1208. [CrossRef]
52. Bridle, T.; Unkovich, I. Critical Factors for Sludge Pyrolysis in Australia. *Water* **2002**, *29*, 43–48.
53. Scholz, W. Paint Additives. In *Surface Coatings: Volume 1 Raw Materials and Their Usage*; Springer: Dordrecht, The Netherlands, 1993; pp. 539–580.
54. Zandersons, J.; Zhurins, A.; Someus, E. Prospects for co-firing of clean coal and creosote-treated waste wood at small-scale power stations. *Therm. Sci.* **2006**, *10*, 109–118. [CrossRef]
55. Nitsos, C.K.; Matis, K.A.; Triantafyllidis, K.S. Optimization of Hydrothermal Pretreatment of Lignocellulosic Biomass in the Bioethanol Production Process. *ChemSusChem* **2013**, *6*, 110–122. [CrossRef]
56. Lee, K.-G.; Lee, S.-E.; Takeoka, G.R.; Kim, J.-H.; Park, B.-S. Antioxidant activity and characterization of volatile constituents of beechwood creosote. *J. Sci. Food Agric.* **2005**, *85*, 1580–1586. [CrossRef]
57. Speight, J.G. *The Chemistry and Technology of Coal*, 3rd ed.; CRC Press: Boca Raton, FL, USA, 2012.
58. Melber, C.; Kielhorn, J.; Mangelsdorf, I.; World Health Organization; The International Programme on Chemical Safety. Coal Tar Creosote. Available online: <https://apps.who.int/iris/handle/10665/42943> (accessed on 15 January 2022).
59. Davis, S.; Boundy, R.G. *Transportation Energy Data Book: Edition 39*; US Department of Energy: Oak Ridge, TN, USA, 2021.
60. Demirbas, A. Higher heating values of lignin types from wood and non-wood lignocellulosic biomasses. *Energy Sources Part A Recovery Util. Environ. Eff.* **2017**, *39*, 592–598. [CrossRef]
61. Christoforou, E.A.; Fokaides, P.A.; Banks, S.W.; Nowakowski, D.; Bridgwater, A.V.; Stefanidis, S.; Kalogiannis, K.G.; Iliopoulou, E.F.; Lappas, A.A. Comparative Study on Catalytic and Non-Catalytic Pyrolysis of Olive Mill Solid Wastes. *Waste Biomass Valorization* **2017**, *9*, 301–313. [CrossRef]
62. Yusuff, A.S.; Adeniyi, O.D.; Olutoye, M.A.; Akpan, U.G. Performance and Emission Characteristics of Diesel Engine Fuelled with Waste Frying Oil Derived Biodiesel-Petroleum Diesel Blend. *Int. J. Eng. Res. Afr.* **2017**, *32*, 100–111. [CrossRef]
63. Jotun, P.E.L. Pioneer Topcoat AV SAFETY DATA SHEET. Available online: https://www.jotun.com/Datasheets/Download?url=%2FSDS%2FSDS__1117__Pioneer%20Topcoat%20AV__Eng__US.pdf (accessed on 19 February 2022).
64. Jotun, P.E.L. Pioneer Topcoat AV Technical Data Sheet. Available online: https://www.jotun.com/Datasheets/Download?url=%2FTDS%2FTDS__1117__Pioneer%20Topcoat%20AV__Eng__US.pdf (accessed on 15 January 2022).
65. Ocampo, C.; Armelin, E.; Liesa, F.; Alemán, C.; Ramis, X.; Iribarren, J.I. Application of a polythiophene derivative as anticorrosive additive for paints. *Prog. Org. Coat.* **2005**, *53*, 217–224. [CrossRef]
66. Meilunas, R.J.; Bentsen, J.G.; Steinberg, A. Analysis of Aged Paint Binders by FTIR Spectroscopy. *Stud. Conserv.* **1990**, *35*, 33–51. [CrossRef]
67. Stringari, C.; Pratt, E. *The Identification and Characterization of Acrylic Emulsion Paint Media*; Saving the Twentieth Century: The Conservation of Modern Materials; Grattan, D., Ed.; Canadian Conservation Institute (CCI): Ottawa, ON, Canada, 1993.
68. Plav, B.; Kobe, S.; Orel, B. Identification of crystallization forms of CaCO₃ with FTIR spectroscopy. *Kovine Zlitine Teh.* **1999**, *33*, 517–521.
69. Nestler, F.H.M. *The Characterization of Wood-Preserving Creosote by Physical and Chemical Methods of Analysis*; U.S. Department of Agriculture, Forest Service, Forest Products Laboratory: Madison, WI, USA, 1974.
70. Iliopoulou, E.F.; Stefanidis, S.D.; Kalogiannis, K.G.; Delimitis, A.; Lappas, A.A.; Triantafyllidis, K.S. Catalytic upgrading of biomass pyrolysis vapors using transition metal-modified ZSM-5 zeolite. *Appl. Catal. B Environ.* **2012**, *127*, 281–290. [CrossRef]
71. Gusev, A.A.; Psarras, A.C.; Triantafyllidis, K.S.; Lappas, A.A.; Diddams, P.A. Effect of Steam Deactivation Severity of ZSM-5 Additives on LPG Olefins Production in the FCC Process. *Molecules* **2017**, *22*, 1784. [CrossRef]
72. Lin, Y.; Zhang, C.; Zhu, L.; Xu, Z.; Gu, M.; Chu, H. Experimental study on pyrolysis of camphor wood catalyzed by CaO-calcined phosphate mixture. *Fuel* **2021**, *288*, 119642. [CrossRef]
73. Iliopoulou, E.F.; Stefanidis, S.; Kalogiannis, K.; Psarras, A.C.; Delimitis, A.; Triantafyllidis, K.S.; Lappas, A.A. Pilot-scale validation of Co-ZSM-5 catalyst performance in the catalytic upgrading of biomass pyrolysis vapours. *Green Chem.* **2014**, *16*, 662–674. [CrossRef]